Characterization of Regenerated Silk Fibroin Membranes for Immobilizing Glucose Oxidase and Construction of a Tetrathiafulvalene-Mediating Glucose Sensor

TONGYIN YU,*[,1] HAIYING LIU,[2] JIAQI DENG,[2] and YONGCHENG LIU[1]

Departments of [1]Macromolecular Science and [2]Chemistry, Fudan University, Shanghai 200433, People's Republic of China

SYNOPSIS

The IR spectra, the electronic absorption bands, and scanning electron microscopy (SEM) of the blend membranes of regenerated silk fibroin and glucose oxidase were reported for the first time and the second generation of glucose sensor based on glucose oxidase immobilized in the regenerated silk fibroin membrane was first constructed. The IR absorption spectra of the pure regenerated silk fibroin membrane were ascribed to its structural characteristics by which the part transition from silk I to silk II was recognized in ethanol immersion. Those spectra of the blend membrane of regenerated silk fibroin and glucose oxidase were identified as a composite of the absorption bands characteristic of both macromolecules. The electronic absorption bands showed that the glucose oxidase in the membrane exists in aggregates. A sea islands' structure was observed by SEM. These findings suggest that the regenerated silk fibroin and glucose oxidase are incompatible and their molecular interactions are very weak. A tetrathiafulvalene-mediating glucose sensor, employing immobilization of glucose oxidase by regenerated silk fibroin, was fabricated. The influences of temperature, applied potential, and pH on steady-state electrocatalytic oxidation of glucose at the sensor were evaluated. The response of the sensor to glucose under N_2 saturation reached 95% steady-state current within 40 s. The sensor could be used repeatedly for 1.5 months without deterioration of the response. © 1995 John Wiley & Sons, Inc.

INTRODUCTION

Over the centuries, silk has been valued as a textile fiber because of its strength, elasticity, softness, luster, absorbency, and affinity for dyes. Bombyx mori silk consists of two types of proteins, fibroin and sericin. Fibroin is the protein that forms the filaments of silkworm silk and gives silk its unique physical and chemical properties. Sericins are a group of gummy proteins that coat the fibroin filaments. Silk fibroin can be used in various forms, such as gels, powders, fibers, or membranes, depending on the method of application. Recently, silk fibroin has been utilized as an immobilization matrix for enzymes.[1-7] As a biomaterial, it has many advantages over other natural or synthetic materials employed in biosensor systems. These include its stability to most solvents including water and good tensile strength and elasticity properties. Its major advantage as an enzyme immobilization matrix is that it entraps the enzymes without using the usual crosslinking chemicals, thus alleviating the problems of residual crosslinking chemicals in the matrix that can deactivate the enzyme's activity. The entrapment process is accomplished by physical, chemical, or mechanical treatment of the membrane (e.g. change in temperature, pH, solvent, mechanical shear or stretch). Bombyx mori silk fibroin has been used as an immobilization matrix for enzymes such as glucose oxidase,[1-4] peroxidase,[5] alkaline phosphatase,[6] and invertase.[7] However, the silk fibroin from Bombyx mori larvae is only available several

* To whom correspondence should be addressed.

Journal of Applied Polymer Science, Vol. 58, 973-980 (1995)
 CCC 0021-8995/95/060973-08

times a year and silk from the silk mill is thought to lose its initial properties due to denaturation of the protein through the high temperature process. Further, the morphology of the enzyme and the reason for retaining the activity of enzymes in the membranes are not known. Moreover, the biosensors coupling immobilized enzymes by Bombyx mori silk fibroin with an oxygen probe or a platinum electrode monitor either the consumption of oxygen or the formation of hydrogen peroxide. Such devices are originally affected by the ambient concentration of oxygen in the sample and require a large overpotential, causing interference. In this article we report that: the regenerated silk fibroin from waste silk can be used to immobilize glucose oxidase; the structure of the blend membrane of the regenerated silk fibroin and glucose oxidase was investigated with IR, scanning electron microscopy (SEM), and electronic absorption bands; and the second generation of the glucose sensor, based on tetrathiafulvalene's shuttling of electrons between the immobilized glucose oxidase in the regenerated silk fibroin membrane and a glass carbon electrode, was constructed.

EXPERIMENTAL

Materials

Glucose oxidase (EC 1.1.3.4, 150,000 U g^{-1}, from Aspergillus niger) and tetrathiafulvalene (TTF) were obtained from Sigma. A solution of Eastman-AQ-55D polymer (28% dispersion) was obtained from Eastman Kodak Co. D-Glucose was purchased from Shanghai Chemical Reagent Company. Glucose solutions were stored overnight to reach mutarotational equilibrium before use. All other chemicals used were of analytical reagent grade.

Regenerated Silk Fibroin Solution

The silk waste of a silk mill was treated with 0.5% $NaHCO_3$ aqueous solution at 100°C for 0.5 h, and then washed with distilled water. The silk was dissolved in 9.3 *M* LiBr aqueous solution. After dialysis against distilled water for 3 days, the solution was filtered and the aqueous solution of silk fibroin was collected.

Membranes were obtained by casting the regenerated silk fibroin solution or the mixture solution of the regenerated silk fibroin and glucose oxidase on glass plates at room temperature in air.

Eastman-AQ-TTF Modified Electrode Construction

The glassy carbon electrode (4 mm in diameter) was polished with 0.1, 0.3, and 0.05 μm Al_2O_3; rinsed thoroughly in deionized water between each polishing step; sonicated in 1 : 1 nitric acid, acetone, and doubly distilled water successively; and dried in air before use. Eastman-AQ-TTF was coated on the electrode by pipetting 8 μL of diluted Eastman-AQ (1 : 25 v/v, Eastman-AQ:acetone) polymer solution containing 0.08 *M* TTF onto the electrode surface and letting it dry in air.

Fabrication of Glucose Sensor

Twenty milligram glucose oxidase in 0.25 mL of silk fibroin solution was completely mixed. Aliquots (8 μL) of the solution were pipetted onto the Eastman-AQ-TTF modified electrode. After being dried in air, the sensor was kept in air at 4°C in a refrigerator.

Glucose Sensor Pretreatment

After the sensor was fabricated and prior to the experiments, the sensor response was stabilized by scanning between +0.45 and −0.2 V (vs. SCE) in 0.1 *M* phosphate buffer (pH 6.7) over 10-min. In this process TTF was oxidized to TTF^+ when the potential was positive enough. Meanwhile, the Na^+ ions in the ester sulfonate group of Eastman-AQ were exchanged with TTF^+ and entered the phosphate buffer. The electrochemical reaction of TTF in the Eastman-AQ film can be described as follows:

$$TTF + SO_3/Na^+ \rightarrow SO_3/TTF^+ + Na^+ + e$$

Measurements

IR spectra were recorded on a FTIR 5DX (Nicolet) spectrometer at room temperature. The spectra of the silk fibroin membrane in the dry state were obtained by the reflection method and those of the glucose oxidase KBr disk were run by the transmission method.

Electronic absorption spectra were measured using a Beckman DU-7 spectrophotometer at room temperature. Air is the reference of all the samples.

SEM was carried out on a Hitachi S-520 operating at 20.0 kV.

Cyclic voltammetry and stationary potential measurements were performed using a FDH 3204 cyclic voltamperograph (Scientific Equipment Co., Fudan University, China) in conjunction with a type

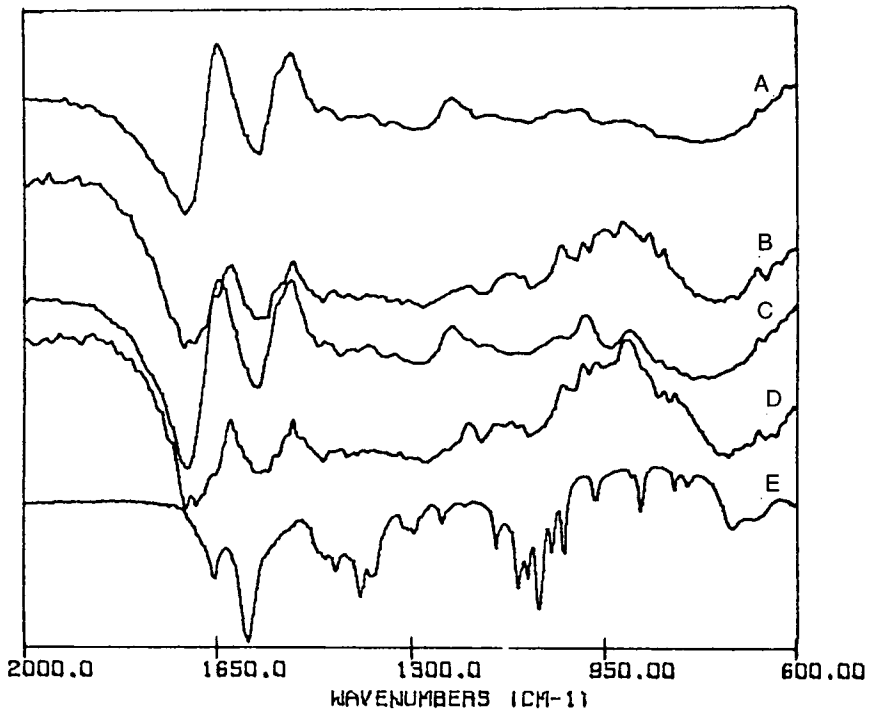

Figure 1 IR spectra of the membranes and KBr disk: (A) silk fibroin membrane; (B) silk fibroin membrane treated with ethanol; (C) silk fibroin membrane containing 7.5% glucose oxidase; (D) silk fibroin membrane containing 7.5% glucose oxidase after treated with ethanol; (E) glucose oxidase KBr disk.

3086 x–y recorder (Yokogawa Hokushin Electric, Tokyo). The three-electrode system consisted of a glucose sensor as the working electrode, a standard calomel reference electrode (SCE), and a platinum wire as the auxiliary electrode. All experiments were conducted in a thermostatted, stirred cell containing 5 mL 0.1M phosphate buffer (pH 7.0) at 30.0 ± 0.5°C. To prevent any competitive oxidation of the reduced glucose oxidase by dissolved oxygen, all solutions were thoroughly degassed by purging with N_2 for at least 10 min prior to use, as were the glucose samples. An oxygen-free environment was maintained at all times during measurements by blanketing the surface of the electrochemical cell with nitrogen. In the constant potential experiments, a constant background current value was obtained before samples of stock glucose solution were added to the buffer solution. Changes in the measured oxidation current were recorded as a function of time following the addition of glucose. The sensor response was measured as the differences between total and residual current.

Table I Electronic Absorption Bands of Membranes Containing Glucose Oxidase and Solution of Glucose Oxidase

State	Concentration (%)	Absorption bands (cm^{-1})
Solution	0.08	450
Solution	0.26	450
Solution	0.29	449, 551, 576
Solution	0.41	449, 551, 576
Solution	1.43	449, 549, 579, 582
Membrane	0.8	476, 484
Membrane	2.1	478, 491
Membrane	7.5	475, 490, 508, 522

RESULTS AND DISCUSSION

Structure Transition of Membranes

Asakura and his coworkers[8,9] employed FTIR (ATR) to determine the conformational transition of the silk fibroin membrane surface treated with methanol on cast membranes. The absorption bands observed for membranes treated with methanol had wave numbers of 1625 (amide I), 1528 (amide II), and 1260 cm^{-1} (amide III), which are characteristic of silk II structure. Membranes without previous

methanol treatment showed absorption bands at 1650 (amide I), 1535 (amide II), and 1235 cm^{-1} (amide III) of the random coil conformation.

Figure 1 shows the IR spectra of the pure regenerated silk fibroin films, blend films, and pure glucose oxidase KBr disk, measured in the range of 2000–600 cm^{-1}. Absorption bands of the regenerated silk fibroin membrane without ethanol treatment are observed at 1706 (amide I), 1571 (amide II), and 1293 cm^{-1} (amide III), characteristic of silk I structure. The membranes treated with ethanol have two groups of absorption bands, one group is 1706 (amide I), 1575 (amide II), and 1312 cm^{-1} (amide III), which are assigned to silk I structure; the other is 1687 (amide I), 1559 (amide II), 1275 cm^{-1} (amide III), characteristic of silk II structure. The conformation transition of regenerated silk fibroin from silk I to silk II is partly completed by ethanol immersion. Compared with the corresponding amide bands of Asakura's membranes, our amide bands have higher wave numbers. In the blend membranes, the absorption bands of glucose oxidase are overlapped. Moreover, no additional absorption bands and no band shift are detected, suggesting that the molecular interactions between the regenerated silk fibroin and glucose oxidase are very weak or even absent in the blend membranes. This may be one of the reasons why glucose oxidase in the films retains its activity.

Morphology of Membranes

The glucose oxidase contains flavin adenine dinucleotide that has a characteristic absorption band at 450 nm. Table I shows that the absorption bands of membranes are different from those of solutions and the aqueous solutions of glucose oxidase always have the absorption band at 450 nm, assigned to the glucose oxidase molecules, of which all the chain segments are unfolded and solvated in the solution. With increasing glucose oxidase concentration up to 0.29%, additional absorption bands appear at 551 and 576 nm; at 1.43% glucose oxidase, the solution has an additional band at 582 nm. The bands shift to longer wavelength (red shift). It is suggested that the glucose oxidase molecules are partly interpenetrating and entangled with one another. The molecular coils and their segments are partly held together by both intramolecular and intermolecular forces such as dispersion, induction, dipole–dipole interaction, and hydrogen bonding. In other words, molecular aggregates of glucose oxidase are formed. The blend membranes of silk fibroin and glucose oxidase do not have the band at 450 nm, but have

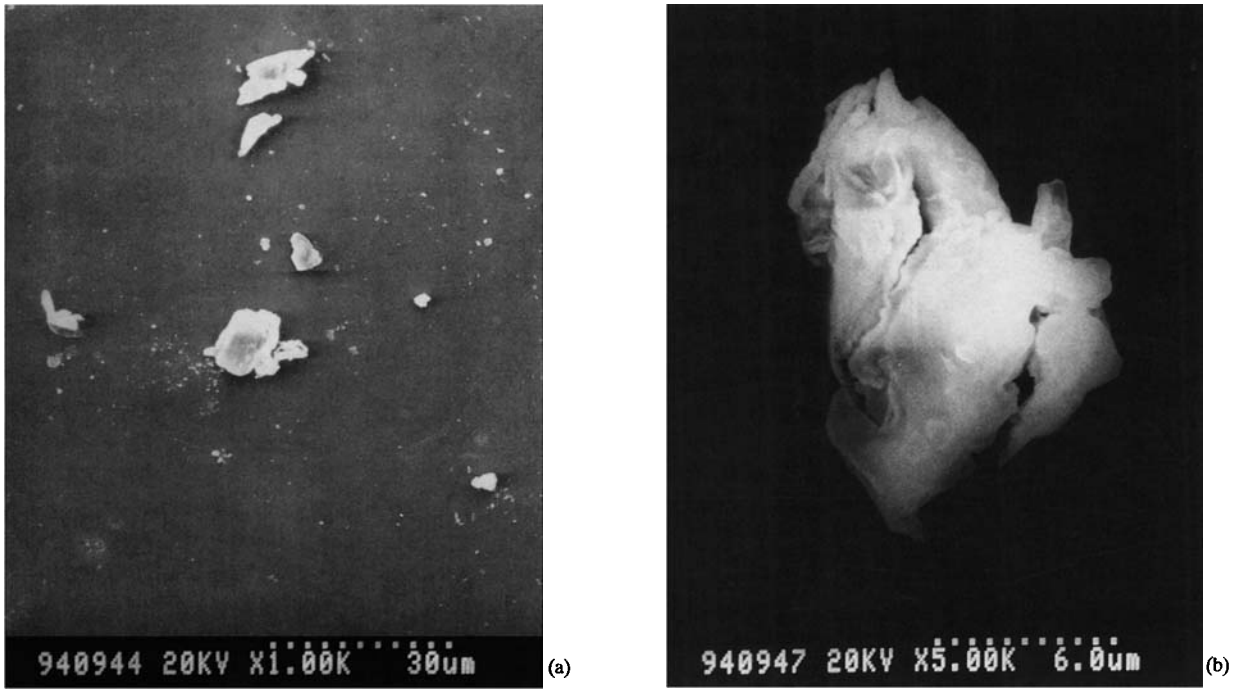

Figure 2 (a, b) Scanning electron microscopy of the silk fibroin membrane containing 0.8% glucose oxidase.

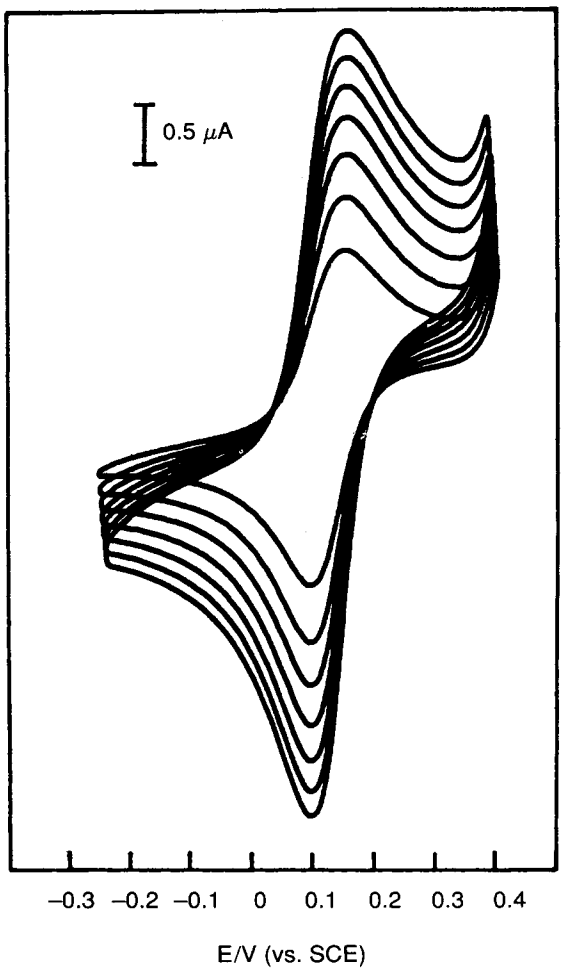

Figure 3 Cyclic voltammograms of the Eastman-AQ-TTF modified glucose sensor reaching steady state at various scan rates (from inner to outer): 25, 45, 65, 85, 105, 125, and 145 mV/s in 0.1*M* phosphate buffer (pH 7.0).

longer than 450-nm bands such as 476, 484, 508, and 522 nm etc. In the process of casting membranes for immobilizing glucose oxidase, the microphase segregation between silk fibroin and glucose oxidase takes place after loss of the solvent and the inversion of a clear one-phase solution into a heterogeneous solution existing in the primary gel. This is attributed to the very weak molecular interactions between silk fibroin and glucose oxidase indicated by the IR spectra. In the glucose oxidase domain, the molecules are in an embroiled state of aggregates, which is consistent with the SEM investigation. As a result, the electronic absorption bands only occur at longer than 450 nm, which are distinct from those of the solution.

SEM (Fig. 2) supports the fact that the glucose oxidase molecules are aggregated in the films. It is obvious that the bright regions are the glucose oxidase domains, which are incompatible with the silk fibroin. The glucose oxidase aggregates are random and in disorder, and are distributed like sea islands, some are larger, some are smaller. The glucose oxidase molecules in the silk fibroin "sea" are fully free due to the very weak molecular interactions between glucose oxidase and silk fibroin. Furthermore, there are empty spaces in the domain, suggesting that the glucose oxidase molecules are not compact; their conformations may be in the most favorable state in which the activity is retained.

Electrochemical Characterization of Glucose Sensor

Cyclic voltammograms of the glucose sensor at different scan rates are shown in Figure 3 in 0.1*M* phosphate buffer (pH 7.0). In the absence of glucose, the enzyme contributes no response and only the electrochemical behavior of TTF in Eastman-AQ polymer is observed. The voltammogram is characteristic of a one-electron process. At a scan rate

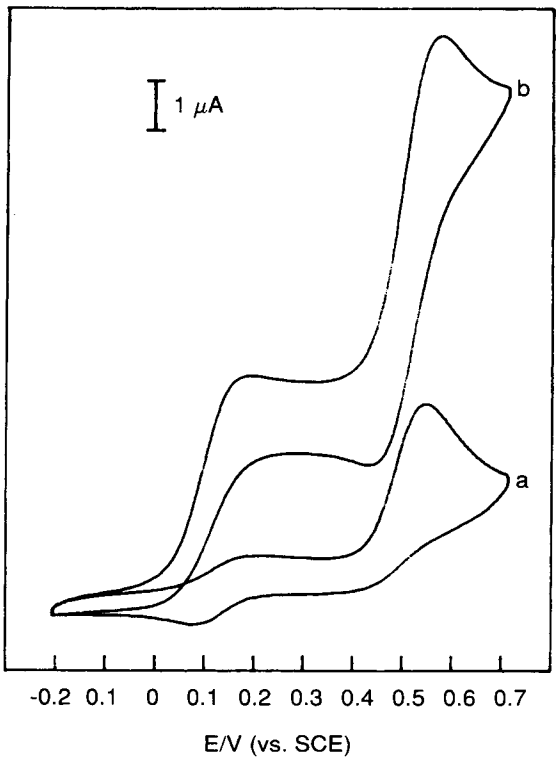

Figure 4 Cyclic voltammograms of the modified glucose sensor with scan potential between −0.2 and +0.7 V at a scan rate of 15 mV/s in 0.1*M* N_2-saturated phosphate buffer (pH 7.0): (a) no glucose, (b) 8 m*M* glucose.

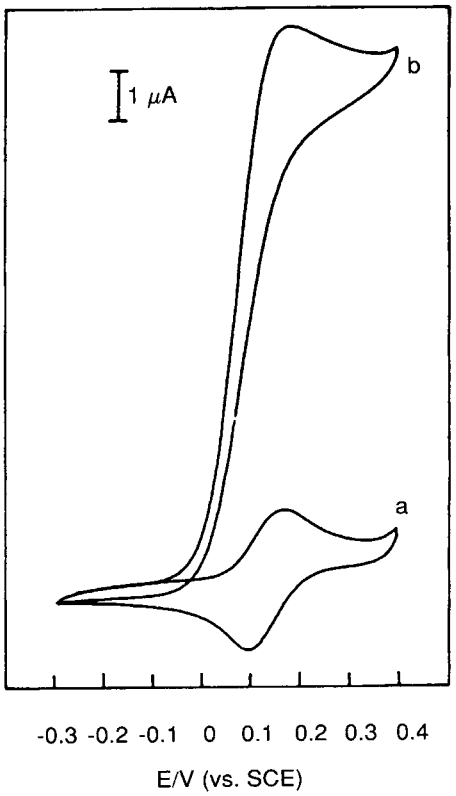

Figure 5 Cyclic voltammograms of the Eastman-AQ-TTF modified glucose sensor with scan potential between −0.2 and +0.4 V at a scan rate of 15 mV/s in 0.1 *M* N_2-saturated phosphate buffer (pH 7.0) in (a) absence of glucose and (b) presence of 9.0 m*M* glucose.

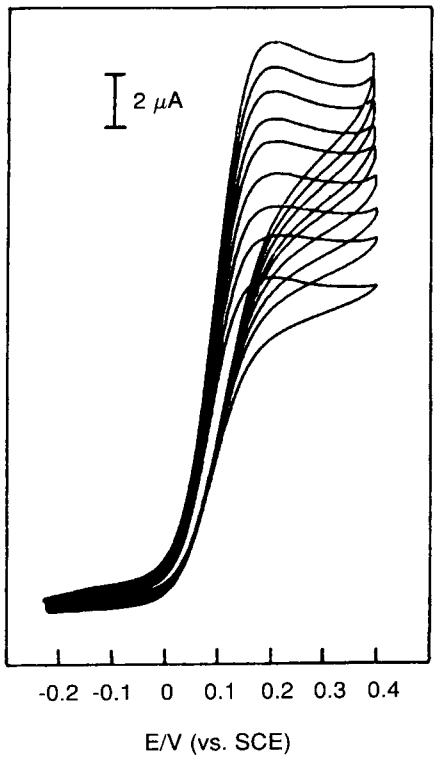

Figure 6 Cyclic voltammograms of the glucose sensor at different speeds in 0.1 *M* N_2-saturated phosphate buffer containing 9.0 m*M* glucose. The scan rates (from inner to outer) are 5, 15, 25, 45, 65, 85, 105, 125, and 145 mV/s, respectively.

below 145 mV/s, almost symmetric waves and less than 60 mV peak-to-peak separations for the oxidation–reduction process display the features of rapid charge transfer of a surface-bound species. The presence of the immobilized enzyme film does not change the electrochemical propriety of the mediator couple.

Electrocatalytic Oxidation of Glucose at Glucose Sensor

The electrochemical behavior of TTF was investigated.[10-12] TTF undergoes two one-electron oxidation processes in aqueous solution yielding TTF^+ and TTF^{2+}. The redox potentials of TTF^+ and TTF^{2+} vary greatly with the method of immobilization and supporting electrolyte used. No electrocatalytic oxidation current is found at the Eastman-AQ-TTF modified electrode when glucose is added to the phosphate buffer. Figure 4(a) is a cyclic voltammogram of the Eastman-AQ-TTF modified glucose sensor in 0.1 *M* phosphate buffer in the absence

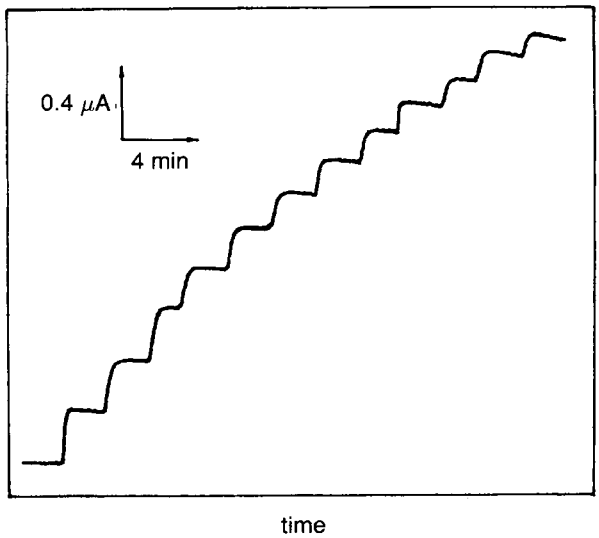

Figure 7 Typical response of the modified glucose sensor to successive increase of 1 m*M* glucose at operating potential +170 mV in the N_2-saturated solution.

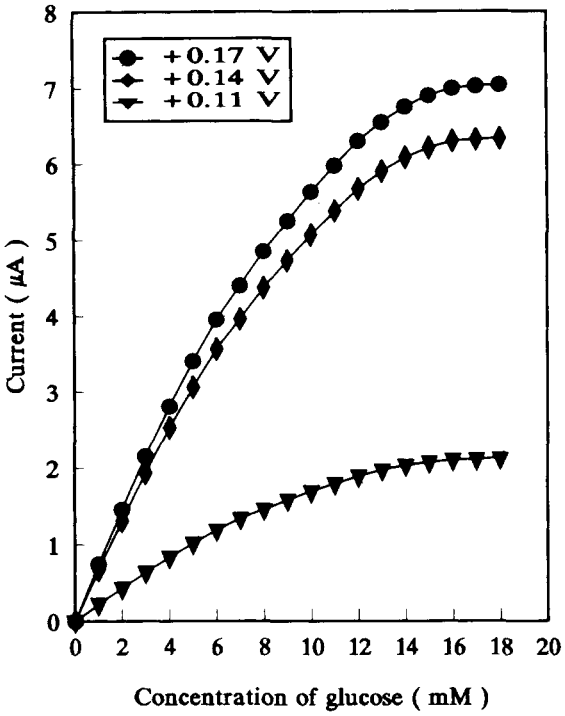

Figure 8 Calibration plot for the glucose sensor, steady-state current was measured in 0.1*M* N_2-saturated phosphate buffer (pH 7.0) at several potentials at 30°C.

of glucose. The cyclic voltammogram of the glucose sensor exhibits two oxidation waves with E_p values of about 150 and 460 mV, respectively. The first cyclic wave (TTF to TTF^+) exhibits reversible electrochemical behavior with a peak separation of 60 mV and the second does not. At the modified glucose sensor, two electrocatalytic oxidation waves are observed with one reduction in the cathodic current upon addition of glucose [Fig. 4(b)], indicating that both TTF^+ and TTF^{2+} can oxidize the $FADH_2$ moiety of glucose oxidase. However, it is better to control the working potential to not exceed +0.40 V because, if not, the system is too complicated and the electroactive species such as urate and ascorbate in biological samples can be readily oxidized at the sensor, thereby producing interference. Figure 5 shows typical cyclic voltammetric results for the sensor with a scan window between −0.20 and +0.40 V. When no glucose is present, the voltammetry shows the usual oxidation and reduction peaks for the TTF. When glucose is added to the solution, the voltammetry changes dramatically, with an accompanying sharp increase in oxidation current and a complete disappearance of reduction current. In comparison to the voltammograms with and without glucose present, it is apparent that TTF can speed up the electron shuttle between the $FAD/FADH_2$ centers of the glucose oxidase immobilized by the regenerated silk fibroin and a glassy carbon electrode.

Figure 6 gives cyclic voltammograms for the glucose sensor in 0.1*M* phosphate buffer containing glucose at various scan speeds. The catalytic current increases with crescent scan rate. The catalytic current is still observable at a higher scan speed. The absence of reduction waves shows that the reproduction rate of TTF from TTF^+ by reaction with $GOD(FADH_2)$ is fast below the scan rate of 145 mV/s. However, at scan rate beyond 200 mV/s, a hysteresis appears and a reduction wave is also observed. The appearance of the hysteresis and the reduction wave are the function of temperature, scan rate, film composition and thickness, substrate concentration, and ionic strength.

Constant Potential Response to Glucose

A typical glucose trace (current vs. time) is shown in Figure 7 for the glucose sensor. The trace plainly displays the quick response and high sensitivity of the glucose sensor to glucose. The time required to arrive at 95% of the steady-state current is less than 40 s after addition of the glucose sample. Figure 8 shows a plot of the current response as a function

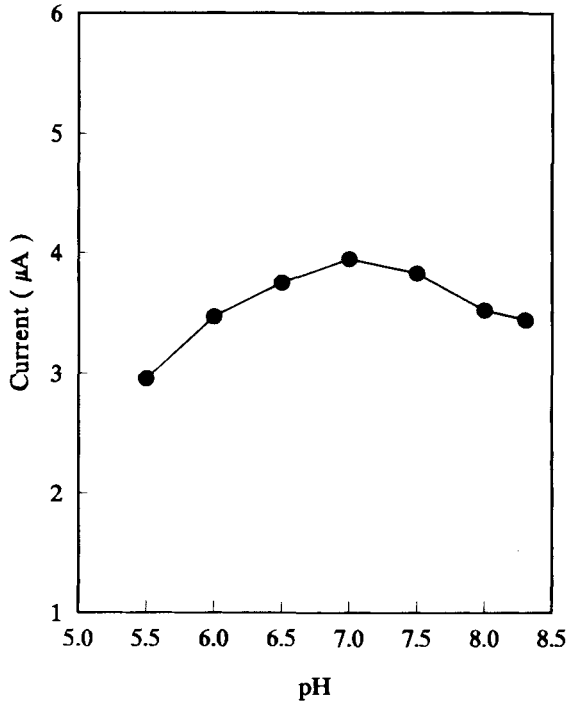

Figure 9 Effect of pH on the glucose sensor. Steady-state current measured in the presence of 6.0*M* glucose in 0.1*M* N_2-saturated phosphate buffer (pH 7.0) at 30°C.

of glucose concentration at various potentials. These results demonstrate that the sensitivity and linear range of detection are functions of the working potential. The highest sensitivity and the linear range are obtained at the potential between 0.17 and 0.30 V. The enhanced linear range and the increased sensitivity with applied potential can be attributed to an increased driving force for the fast reoxidation of the $FADH_2$ of glucose oxidase.

Effects of pH and Temperature on Glucose Sensor

The pH dependence of the electrocatalytic current was measured at 4.0 m*M* glucose concentration in N_2-saturated solution (Fig. 9). The substrate response exhibits an optimum at a broader pH 6.5–8.0 and reaches maximum at pH 7.0. However, extreme pH will cause irreversible denaturation of the enzyme.

The effect of temperature on the sensor has been examined between 15 and 60°C. At 50°C, the immobilized enzyme loses 10% of its activity in 180 min. The experiment shows that the steady-state current response increases with temperature, arriving at a maximum value at about 55°C. With temperature beyond 55°C, the response declines rapidly owing to the denaturation of the enzyme.

Reproducibility and Storage Stability of Sensor

The sensor displayed good reproducibility and the relative standard deviations of nine repetitive measurements were 2.2 and 2.5% for the solution of 2.0 and 6.0 m*M* glucose, respectively. After 80 measurements, the standard deviation of response was within 4%. The lifetime of the sensor was measured by keeping it in air at 4°C, and response of the sensor to glucose was determined at 3-day intervals. The sensor displayed good storage characteristics for the current response maintained almost unchanged for 1.5 months.

CONCLUSIONS

It is feasible that the regenerated silk fibroin is utilized as an immobilization matrix of glucose oxidase. The IR spectra of the blend membrane of the regenerated silk fibroin and glucose oxidase indicate that the enzyme does not much affect the structure of the regenerated silk fibroin and that the partial molecular conformational transition from silk I to silk II in the film occurs after ethanol immersion. The enzyme in the blend membrane is found to be in the form of molecular aggregates with SEM and electronic absorption spectra. The TTF can efficiently facilitate electron transfer between the FAD/$FADH_2$ coenzymes of the immobilized glucose oxidase silk fibroin and a glassy carbon electrode. The protective effect of regenerated silk fibroin for glucose oxidase against autoinactivation and thermodeactivation can be ascribed to a close molding of the structure of the enzyme with regenerated silk fibroin. The good stability of this sensor and its ease of construction hold great promise for practical application in bioanalysis.

This work was supported by the National Science Foundation of China and the Electroanalytical Chemistry Open Laboratory of Changchun Institute of Applied Chemistry, Chinese Academy of Sciences.

REFERENCES

1. A. Kuzuhara, T. Asakura, R. Tomoda, and T. J. Matsunaga, *J. Biotechnol.*, **5,** 199 (1987).
2. T. Asakura, H. Yoshimizu, A. Kuzuhara, and T. J. Matsunaga, *J. Sericin Sci. Jpn.*, **57,** 203 (1988).
3. M. Demura and T. Asakura, *Biotechnol. Bioeng.*, **33,** 598 (1989).
4. M. Demura, T. Asakura, and T. Kurso, *Biosensors*, **4,** 361 (1989).
5. M. Demura, T. Asakura, E. Nakamura, and H. Tamura, *J. Biotechnol.*, **10,** 113 (1989).
6. T. Asakura, J. Kanetake, and M. Demura, *Poly-Plast. Technol. Eng.*, **28,** 453 (1989).
7. H. Yoshimizu and T. Asakura, *J. Appl. Poly. Sci.*, **40,** 127 (1990).
8. T. Asakura, and H. Yoshimizu, *J. Appl. Poly. Sci.*, **40,** 1745 (1990).
9. T. Asakura, A. Kuzuhara, R. Tabeta, and H. Saito, *Macromolecules*, **18,** 1841 (1985).
10. K. N. Kuo, P. R. Moses, J. R. Lenhard, D. C. Green, and R. W. Murray, *Anal. Chem.*, **51,** 745 (1979).
11. M. Kamche, H. Menet, and A. Moradpour, *J. Am. Chem. Soc.*, **104,** 4520 (1982).
12. J. D. Norton, W. E. Benson, H. S. White, B. D. Pendley, and H. D. Abruna, *Anal. Chem.*, **63,** 1909 (1991).

Received December 20, 1994
Accepted April 18, 1995